

Higgs Decay to Top Quarks at $\mathcal{O}(\alpha_s^2)$ R. Harlander^a and M. Steinhauser^b

^a*Institut für Theoretische Teilchenphysik, Universität Karlsruhe,
D-76128 Karlsruhe, Germany.*

^b*Max-Planck-Institut für Physik, Werner-Heisenberg-Institut,
D-80805 Munich, Germany*

Abstract

Three-loop corrections to the scalar and pseudo-scalar current correlator are calculated. By applying the large momentum expansion mass terms up to order $(m^2/q^2)^4$ are evaluated analytically. As an application $\mathcal{O}(\alpha_s^2)$ corrections to the decay of a scalar and pseudo-scalar Higgs boson into top quarks are considered. It is shown that for a Higgs mass not far above the $t\bar{t}$ threshold these higher order mass corrections are necessary to get reliable results.

PACS numbers: 12.38.-t, 14.65.Ha, 14.80.Bn, 14.80.Cp.

*The complete postscript file of this preprint, including figures, is available via anonymous ftp at www-ttp.physik.uni-karlsruhe.de (129.13.102.139) as `/ttp97-12/ttp97-12.ps` or via www at <http://www-ttp.physik.uni-karlsruhe.de/cgi-bin/preprints>.

1 Introduction and notation

A crucial question in elementary particle physics is whether nature makes use of the spontaneous symmetry breaking for generating the masses or not. In the minimal standard model (SM) this mechanism requires the existence of a scalar particle, the Higgs boson. Extensions of the SM, e.g. models with more than one Higgs doublet or supersymmetric versions of the SM, predict also pseudo-scalar Higgs bosons, A .

However, up to now there is no experimental evidence for such a particle and the direct search at LEP via the process $e^+e^- \rightarrow f\bar{f}H$ rules out the mass range $M_H \leq 65.6$ GeV with a 95% confidence level (CL) [1]. Assuming the validity of the SM the precision data are sensitive to the Higgs boson and a recent global fit yields $M_H = 149_{-82}^{+148}$ GeV together with a 95% CL upper bound of 550 GeV [2] (in this context see also [3]). Theoretical arguments based on unitarity or the validity of perturbation theory request an upper limit on the Higgs mass of about 1 TeV.

In this paper we consider the decay of a Higgs boson, scalar or pseudo-scalar, with mass above 400 GeV, into a top-antitop quark pair. Since the velocity of one of the quarks for this mass range is $v \gtrsim 0.5$, threshold effects can safely be neglected and the decay rate can be treated in a purely perturbative way. The full mass dependence for this process is only known to $\mathcal{O}(\alpha_s)$ [4], while to order α_s^2 only mass terms up to $M_t^2/M_{H/A}^2$ are available [5, 6, 7, 8], where M_t is the top quark mass, and they show up to be quite sizeable [6]. $\mathcal{O}(\alpha_s^3)$ corrections have recently been evaluated in the massless case [9].

In the following, making use of a technique recently developed for the automatic computation of mass corrections to the vector current correlator [10, 11], we will demonstrate that the inclusion of mass terms up to order $(M_t^2/M_{H/A}^2)^4$ leads to reliable results at $\mathcal{O}(\alpha_s^2)$ in the considered mass range. We note that the results presented in this paper for the decay into top quarks may be generalized to any fermion species. However, even for bottom quarks already the quadratic mass corrections are very small.

To fix the notation we define:

$$q^2 \Pi^\delta(q^2) = i \int dx e^{iqx} \langle 0 | T j^\delta(x) j^\delta(0) | 0 \rangle, \quad \text{with } \delta \in \{s, p\} \quad (1)$$

where $\Pi^s(q^2)$ ($\Pi^p(q^2)$) represents the scalar (pseudo-scalar) current correlator in momentum space. The currents are given by

$$j^s = \bar{\psi}\psi, \quad j^p = i\bar{\psi}\gamma_5\psi. \quad (2)$$

It should be noted that as far as renormalization is concerned it is convenient to consider the combination $m j^\delta$ in the on-shell scheme and $\bar{m} j^\delta$ in the $\overline{\text{MS}}$ scheme, where m (\bar{m}) is the generic pole ($\overline{\text{MS}}$) mass, in order to avoid additional renormalization constants. The physical observable $R^\delta(s)$ is related to $\Pi^\delta(q^2)$ via the relation

$$R^\delta(s) = 8\pi \text{Im} \Pi^\delta(q^2 = s + i\epsilon). \quad (3)$$

The current correlator can be written as

$$\Pi^\delta(q^2) = \Pi^{(0),\delta}(q^2) + \frac{\alpha_s(\mu^2)}{\pi} C_F \Pi^{(1),\delta}(q^2) + \left(\frac{\alpha_s(\mu^2)}{\pi} \right)^2 \Pi^{(2),\delta}(q^2) + \dots, \quad (4)$$

$$\Pi^{(2),\delta} = C_F^2 \Pi_A^{(2),\delta} + C_A C_F \Pi_{NA}^{(2),\delta} + C_F T n_l \Pi_l^{(2),\delta} + C_F T \Pi_F^{(2),\delta} + C_F T \Pi_S^{(2),\delta}, \quad (5)$$

and similarly for $R^\delta(s)$. The normalization in Eq. (3) guarantees that $R^{(0),\delta}(s) \rightarrow 3$ for $s \rightarrow \infty$. The colour factors ($C_F = (N_c^2 - 1)/(2N_c)$ and $C_A = N_c$) correspond to the Casimir operators of the fundamental and adjoint representations, respectively. For the numerical evaluation we set $N_c = 3$. The trace normalization of the fundamental representation is $T = 1/2$. The number of light (massless) quark flavours is denoted by n_l .

In Eq. (5) $\Pi_A^{(2),\delta}$ is the abelian contribution which also exists in QED, and $\Pi_{NA}^{(2),\delta}$ results from the non-abelian structure specific for QCD. The contribution of diagrams containing a second massless or massive quark loop is denoted by $\Pi_l^{(2),\delta}$ and $\Pi_F^{(2),\delta}$, respectively. $\Pi_S^{(2),\delta}$ represents the terms arising from the double-triangle diagram and is called the singlet contribution. The case for the double-bubble diagram where the inner quark mass is much heavier than the outer one is not listed as it does not contribute in cases of physical interest.

The outline of the paper is as follows: In Section 2 the method is briefly described and the results for the correlator functions are given. In Section 3 mass effects for the decay of a scalar and pseudo-scalar Higgs particle into top quarks are presented and the results are discussed.

2 Results for the current correlators

In this section we keep the discussion general and consider the scalar and pseudo-scalar current correlators with a generic quark mass m . In Section 3 the specification to the case $m = M_t$ is performed and numerical values are given.

Let us in a first step outline the main ideas of the large momentum expansion and its realization by a computer¹. The large momentum procedure [12] requires the identification of certain subgraphs associated with the Feynman diagram to be calculated. These subgraphs then have to be expanded in their small dimensional quantities (i.e. all except the large momenta) and the resulting terms, being products of tadpoles and massless integrals, have to be calculated. The number of these terms increases rapidly with the number of loops. In our case of a massive current correlator, the one- and two-loop diagrams generate 17 terms altogether, so that they still can be treated by hand. In the three-loop case, however, there are 19 topologies, contributing 266 terms, and their generation by hand is not feasible. Therefore we completely automated the large momentum procedure for massive two-point functions and directly fed the generated terms to the FORM [13] packages MATAD and MINCER [14]. After calculating the single terms the results of all diagrams were added giving a finite expression after renormalization.

We are now prepared to present the result. Let us first consider the scalar correlator. The results for the different contributions read in the $\overline{\text{MS}}$ scheme ($l_{qm} \equiv \ln(-q^2/\bar{m}^2)$, $l_{q\mu} \equiv$

¹ For a more detailed discussion see Ref. [11].

$\ln(-q^2/\mu^2)$:

$$\begin{aligned}\bar{\Pi}^{(0),s} &= \frac{3}{16\pi^2} \left\{ 4 - 2l_{q\mu} + \frac{\bar{m}^2}{q^2} \left[-16 + 12l_{q\mu} \right] + \left(\frac{\bar{m}^2}{q^2} \right)^2 \left[-18 - 12l_{qm} \right] \right. \\ &\quad \left. + \left(\frac{\bar{m}^2}{q^2} \right)^3 \left[\frac{4}{3} - 8l_{qm} \right] + \left(\frac{\bar{m}^2}{q^2} \right)^4 \left[7 - 12l_{qm} \right] \right\} + \dots, \quad (6)\end{aligned}$$

$$\begin{aligned}\bar{\Pi}^{(1),s} &= \frac{3}{16\pi^2} \left\{ \frac{131}{8} - 6\zeta_3 - \frac{17}{2}l_{q\mu} + \frac{3}{2}l_{q\mu}^2 \right. \\ &\quad \left. + \frac{\bar{m}^2}{q^2} \left[-94 + 36\zeta_3 + 60l_{q\mu} - 18l_{q\mu}^2 \right] \right. \\ &\quad \left. + \left(\frac{\bar{m}^2}{q^2} \right)^2 \left[-44 - 48\zeta_3 - 69l_{qm} - 18l_{qm}^2 + (63 + 54l_{qm})l_{q\mu} \right] \right. \\ &\quad \left. + \left(\frac{\bar{m}^2}{q^2} \right)^3 \left[-\frac{461}{9} - \frac{956}{9}l_{qm} - \frac{98}{3}l_{qm}^2 + (-20 + 48l_{qm})l_{q\mu} \right] \right. \\ &\quad \left. + \left(\frac{\bar{m}^2}{q^2} \right)^4 \left[\frac{8263}{144} - \frac{881}{6}l_{qm} - \frac{135}{2}l_{qm}^2 + \left(-\frac{141}{2} + 90l_{qm} \right)l_{q\mu} \right] \right\} + \dots, \quad (7)\end{aligned}$$

$$\begin{aligned}\bar{\Pi}_A^{(2),s} &= \frac{3}{16\pi^2} \left\{ \frac{1613}{64} - 24\zeta_3 + \frac{9}{4}\zeta_4 + 15\zeta_5 + \left(-\frac{691}{32} + \frac{9}{2}\zeta_3 \right)l_{q\mu} + \frac{105}{16}l_{q\mu}^2 - \frac{3}{4}l_{q\mu}^3 \right. \\ &\quad \left. + \frac{\bar{m}^2}{q^2} \left[-\frac{3471}{16} + 220\zeta_3 - 18\zeta_4 - 130\zeta_5 \right. \right. \\ &\quad \left. \left. + \left(\frac{1911}{8} - 72\zeta_3 \right)l_{q\mu} - \frac{369}{4}l_{q\mu}^2 + 18l_{q\mu}^3 \right] \right. \\ &\quad \left. + \left(\frac{\bar{m}^2}{q^2} \right)^2 \left[-\frac{4517}{32} - 340\zeta_3 + 72\zeta_4 + 115\zeta_5 - 12B_4 \right. \right. \\ &\quad \left. \left. + \left(-\frac{2871}{16} + 27\zeta_3 \right)l_{qm} - \frac{315}{4}l_{qm}^2 - 18l_{qm}^3 \right. \right. \\ &\quad \left. \left. + \left(\frac{819}{8} + 216\zeta_3 + \frac{1053}{4}l_{qm} + 81l_{qm}^2 \right)l_{q\mu} + \left(-\frac{405}{4} - \frac{243}{2}l_{qm} \right)l_{q\mu}^2 \right] \right. \\ &\quad \left. + \left(\frac{\bar{m}^2}{q^2} \right)^3 \left[-\frac{48895}{1944} - 427\zeta_3 + 48\zeta_4 - 80\zeta_5 - 8B_4 \right. \right. \\ &\quad \left. \left. + \left(-\frac{8938}{27} - 116\zeta_3 \right)l_{qm} - \frac{1375}{6}l_{qm}^2 - \frac{1639}{27}l_{qm}^3 \right. \right. \\ &\quad \left. \left. + \left(\frac{291}{2} + \frac{1636}{3}l_{qm} + 196l_{qm}^2 \right)l_{q\mu} + (96 - 144l_{qm})l_{q\mu}^2 \right] \right. \\ &\quad \left. + \left(\frac{\bar{m}^2}{q^2} \right)^4 \left[-\frac{6460859}{31104} - 60\zeta_3 + 72\zeta_4 - 40\zeta_5 - 12B_4 \right. \right. \\ &\quad \left. \left. + \left(-\frac{1242845}{1296} - 173\zeta_3 \right)l_{qm} - \frac{546029}{864}l_{qm}^2 - \frac{32735}{216}l_{qm}^3 \right. \right.\end{aligned}$$

$$+ \left(-\frac{63305}{96} + 910 l_{qm} + \frac{2025}{4} l_{qm}^2 \right) l_{q\mu} + \left(\frac{2655}{8} - \frac{675}{2} l_{qm} \right) l_{q\mu}^2 \Big] \Big\} + \dots, (8)$$

$$\begin{aligned} \bar{\Pi}_{NA}^{(2),s} = & \frac{3}{16\pi^2} \left\{ \frac{14419}{288} - \frac{75}{4} \zeta_3 - \frac{9}{8} \zeta_4 - \frac{5}{2} \zeta_5 + \left(-\frac{893}{32} + \frac{31}{4} \zeta_3 \right) l_{q\mu} + \frac{71}{12} l_{q\mu}^2 - \frac{11}{24} l_{q\mu}^3 \right. \\ & + \frac{\bar{m}^2}{q^2} \left[-\frac{12617}{48} + 90 \zeta_3 + 9 \zeta_4 + 15 \zeta_5 \right. \\ & \left. + \left(\frac{4601}{24} - 51 \zeta_3 \right) l_{q\mu} - \frac{207}{4} l_{q\mu}^2 + \frac{11}{2} l_{q\mu}^3 \right] \\ & + \left(\frac{\bar{m}^2}{q^2} \right)^2 \left[-\frac{50347}{288} + \frac{467}{12} \zeta_3 - 36 \zeta_4 - \frac{95}{2} \zeta_5 + 6 B_4 \right. \\ & + \left(-\frac{9503}{48} + \frac{27}{2} \zeta_3 \right) l_{qm} - 38 l_{qm}^2 - \frac{11}{2} l_{qm}^3 \\ & + \left(\frac{3005}{24} + 44 \zeta_3 + 136 l_{qm} + \frac{33}{2} l_{qm}^2 \right) l_{q\mu} + \left(-\frac{231}{8} - \frac{99}{4} l_{qm} \right) l_{q\mu}^2 \Big] \\ & + \left(\frac{\bar{m}^2}{q^2} \right)^3 \left[-\frac{61601}{972} + \frac{7}{2} \zeta_3 - 24 \zeta_4 + 20 \zeta_5 + 4 B_4 \right. \\ & + \left(-\frac{208093}{648} + 8 \zeta_3 \right) l_{qm} - \frac{563}{6} l_{qm}^2 - \frac{521}{54} l_{qm}^3 \\ & + \left(\frac{2161}{108} + \frac{4375}{27} l_{qm} + \frac{539}{18} l_{qm}^2 \right) l_{q\mu} + \left(\frac{55}{6} - 22 l_{qm} \right) l_{q\mu}^2 \Big] \\ & + \left(\frac{\bar{m}^2}{q^2} \right)^4 \left[\frac{396607}{1296} - \frac{1393}{24} \zeta_3 - 36 \zeta_4 + 10 \zeta_5 + 6 B_4 \right. \\ & + \left(-\frac{368443}{864} + 63 \zeta_3 \right) l_{qm} - \frac{57929}{288} l_{qm}^2 - \frac{803}{24} l_{qm}^3 \\ & \left. + \left(-\frac{255017}{1728} + \frac{18421}{72} l_{qm} + \frac{495}{8} l_{qm}^2 \right) l_{q\mu} + \left(\frac{517}{16} - \frac{165}{4} l_{qm} \right) l_{q\mu}^2 \right] \Big\} + \dots, \end{aligned} \quad (9)$$

$$\begin{aligned} \bar{\Pi}_l^{(2),s} = & \frac{3}{16\pi^2} \left\{ -\frac{511}{36} + 4 \zeta_3 + \left(\frac{65}{8} - 2 \zeta_3 \right) l_{q\mu} - \frac{11}{6} l_{q\mu}^2 + \frac{1}{6} l_{q\mu}^3 \right. \\ & + \frac{\bar{m}^2}{q^2} \left[\frac{817}{12} - 12 \zeta_3 + \left(-\frac{313}{6} + 12 \zeta_3 \right) l_{q\mu} + 15 l_{q\mu}^2 - 2 l_{q\mu}^3 \right] \\ & + \left(\frac{\bar{m}^2}{q^2} \right)^2 \left[\frac{3311}{72} - \frac{4}{3} \zeta_3 + \frac{595}{12} l_{qm} + 10 l_{qm}^2 + 2 l_{qm}^3 \right. \\ & + \left(-\frac{193}{6} - 16 \zeta_3 - 38 l_{qm} - 6 l_{qm}^2 \right) l_{q\mu} + \left(\frac{21}{2} + 9 l_{qm} \right) l_{q\mu}^2 \Big] \\ & + \left(\frac{\bar{m}^2}{q^2} \right)^3 \left[-\frac{8347}{486} + \frac{80}{3} \zeta_3 + \frac{4534}{81} l_{qm} + \frac{149}{9} l_{qm}^2 + \frac{62}{27} l_{qm}^3 \right. \\ & \left. + \left(-\frac{311}{27} - \frac{1316}{27} l_{qm} - \frac{98}{9} l_{qm}^2 \right) l_{q\mu} + \left(-\frac{10}{3} + 8 l_{qm} \right) l_{q\mu}^2 \right] \Big\} \end{aligned}$$

$$\begin{aligned}
& + \left(\frac{\bar{m}^2}{q^2} \right)^4 \left[-\frac{54461}{1296} + 20 \zeta_3 + \frac{2821}{27} l_{qm} + \frac{287}{8} l_{qm}^2 + \frac{25}{6} l_{qm}^3 \right. \\
& \quad \left. + \left(\frac{16723}{432} - \frac{1331}{18} l_{qm} - \frac{45}{2} l_{qm}^2 \right) l_{q\mu} + \left(-\frac{47}{4} + 15 l_{qm} \right) l_{q\mu}^2 \right] \} + \dots , \quad (10)
\end{aligned}$$

$$\begin{aligned}
\bar{\Pi}_F^{(2),s} &= \frac{3}{16\pi^2} \left\{ -\frac{511}{36} + 4 \zeta_3 + \left(\frac{65}{8} - 2 \zeta_3 \right) l_{q\mu} - \frac{11}{6} l_{q\mu}^2 + \frac{1}{6} l_{q\mu}^3 \right. \\
& + \frac{\bar{m}^2}{q^2} \left[\frac{881}{12} - 12 \zeta_3 + \left(-\frac{385}{6} + 12 \zeta_3 \right) l_{q\mu} + 15 l_{q\mu}^2 - 2 l_{q\mu}^3 \right] \\
& + \left(\frac{\bar{m}^2}{q^2} \right)^2 \left[\frac{9863}{72} - \frac{94}{3} \zeta_3 + \frac{1135}{12} l_{qm} + \frac{23}{2} l_{qm}^2 + 2 l_{qm}^3 \right. \\
& \quad \left. + \left(-\frac{193}{6} - 16 \zeta_3 - 38 l_{qm} - 6 l_{qm}^2 \right) l_{q\mu} + \left(\frac{21}{2} + 9 l_{qm} \right) l_{q\mu}^2 \right] \\
& + \left(\frac{\bar{m}^2}{q^2} \right)^3 \left[\frac{10757}{486} - \frac{628}{9} \zeta_3 + \frac{4316}{27} l_{qm} + \frac{1195}{27} l_{qm}^2 + \frac{124}{27} l_{qm}^3 \right. \\
& \quad \left. + \left(-\frac{311}{27} - \frac{1316}{27} l_{qm} - \frac{98}{9} l_{qm}^2 \right) l_{q\mu} + \left(-\frac{10}{3} + 8 l_{qm} \right) l_{q\mu}^2 \right] \\
& + \left(\frac{\bar{m}^2}{q^2} \right)^4 \left[-\frac{193831}{864} - 187 \zeta_3 + \frac{13051}{72} l_{qm} + \frac{7699}{72} l_{qm}^2 + \frac{47}{3} l_{qm}^3 \right. \\
& \quad \left. + \left(\frac{16723}{432} - \frac{1331}{18} l_{qm} - \frac{45}{2} l_{qm}^2 \right) l_{q\mu} + \left(-\frac{47}{4} + 15 l_{qm} \right) l_{q\mu}^2 \right] \} + \dots , \quad (11)
\end{aligned}$$

$$\begin{aligned}
\bar{\Pi}_S^{(2),s} &= \frac{3}{16\pi^2} \left\{ \frac{\bar{m}^2}{q^2} \left[\frac{236}{3} - 40 \zeta_3 - 20 \zeta_5 - 24 l_{q\mu} \right] \right. \\
& + \left(\frac{\bar{m}^2}{q^2} \right)^2 \left[-84 + 8 \zeta_3 + 160 \zeta_5 + (-36 + 72 \zeta_3) l_{qm} \right] \\
& + \left(\frac{\bar{m}^2}{q^2} \right)^3 \left[\frac{37}{8} - 62 \zeta_3 + 320 \zeta_5 + \left(-\frac{3}{4} - 36 \zeta_3 \right) l_{qm} + 33 l_{qm}^2 + 12 l_{qm}^3 \right] \\
& + \left(\frac{\bar{m}^2}{q^2} \right)^4 \left[\frac{178423}{243} - \frac{4472}{9} \zeta_3 + \left(\frac{22289}{81} + 16 \zeta_3 \right) l_{qm} \right. \\
& \quad \left. - 26 l_{qm}^2 - \frac{28}{3} l_{qm}^3 \right] \} + \dots , \quad (12)
\end{aligned}$$

where ζ is Riemann's zeta function with values $\zeta_2 = \pi^2/6$, $\zeta_3 \approx 1.20206$, $\zeta_4 = \pi^4/90$ and $\zeta_5 \approx 1.03693$. The constant B_4 is typical for three-loop tadpole integrals and is given by $B_4 \approx -1.76280$ [15]. The corresponding results in the on-shell scheme are obtained by substituting in the combination $\bar{m}^2 \bar{\Pi}(q^2)$ the $\overline{\text{MS}}$ mass, \bar{m} , w.r.t. the on-shell mass [16].

For the pseudo-scalar current correlator a minor complication arises in connection with γ_5 . While the non-singlet contribution allows the use of the anticommuting definition, for the singlet diagram we take the prescription for γ_5 introduced in [17]. Thereby we follow

the strategy outlined in [18, 7] and replace γ_5 in the vertices according to

$$\gamma_5 \rightarrow \frac{i}{4!} \varepsilon_{\mu\nu\rho\sigma} \gamma^{[\mu\nu\rho\sigma]}, \quad (13)$$

where $\gamma^{[\mu\nu\rho\sigma]}$ represents the antisymmetrized product of four γ -matrices and may be written as

$$\gamma^{[\mu\nu\rho\sigma]} = \frac{1}{4} (\gamma^\mu \gamma^\nu \gamma^\rho \gamma^\sigma + \gamma^\sigma \gamma^\rho \gamma^\nu \gamma^\mu - \gamma^\nu \gamma^\rho \gamma^\sigma \gamma^\mu - \gamma^\mu \gamma^\sigma \gamma^\rho \gamma^\nu). \quad (14)$$

Because the double-triangle diagram contains no sub-divergencies and consequently has a finite imaginary part it is allowed to contract the new polarization tensor with eight indices with the product of four metric tensors and compute the scalar integrals in the same way as for the non-singlet contributions. Even more, in contrast to the scalar case $\bar{\Pi}_S^{(2),p}$ is finite from the very beginning.

The results for the pseudo-scalar case read:

$$\begin{aligned} \bar{\Pi}^{(0),p} &= \frac{3}{16\pi^2} \left\{ 4 - 2l_{q\mu} + 4\frac{\bar{m}^2}{q^2} l_{q\mu} + \left(\frac{\bar{m}^2}{q^2}\right)^2 \left[-2 + 4l_{qm} \right] \right. \\ &\quad \left. + \left(\frac{\bar{m}^2}{q^2}\right)^3 \left[-\frac{20}{3} + 8l_{qm} \right] + \left(\frac{\bar{m}^2}{q^2}\right)^4 \left[-\frac{59}{3} + 20l_{qm} \right] \right\} + \dots, \quad (15) \end{aligned}$$

$$\begin{aligned} \bar{\Pi}^{(1),p} &= \frac{3}{16\pi^2} \left\{ \frac{131}{8} - 6\zeta_3 - \frac{17}{2} l_{q\mu} + \frac{3}{2} l_{q\mu}^2 + \frac{\bar{m}^2}{q^2} \left[-6 + 12\zeta_3 + 4l_{q\mu} - 6l_{q\mu}^2 \right] \right. \\ &\quad \left. + \left(\frac{\bar{m}^2}{q^2}\right)^2 \left[4 + 27l_{qm} + 6l_{qm}^2 + (15 - 18l_{qm}) l_{q\mu} \right] \right. \\ &\quad \left. + \left(\frac{\bar{m}^2}{q^2}\right)^3 \left[-\frac{515}{9} + \frac{628}{9} l_{qm} + \frac{82}{3} l_{qm}^2 + (52 - 48l_{qm}) l_{q\mu} \right] \right. \\ &\quad \left. + \left(\frac{\bar{m}^2}{q^2}\right)^4 \left[-\frac{36985}{144} + \frac{3101}{18} l_{qm} + \frac{539}{6} l_{qm}^2 + \left(\frac{355}{2} - 150l_{qm}\right) l_{q\mu} \right] \right\} + \dots, \quad (16) \end{aligned}$$

$$\begin{aligned} \bar{\Pi}_A^{(2),p} &= \frac{3}{16\pi^2} \left\{ \frac{1613}{64} - 24\zeta_3 + \frac{9}{4} \zeta_4 + 15\zeta_5 + \left(-\frac{691}{32} + \frac{9}{2} \zeta_3\right) l_{q\mu} + \frac{105}{16} l_{q\mu}^2 - \frac{3}{4} l_{q\mu}^3 \right. \\ &\quad \left. + \frac{\bar{m}^2}{q^2} \left[\frac{1697}{48} + 54\zeta_3 - 6\zeta_4 - 70\zeta_5 + \left(\frac{13}{8} - 24\zeta_3\right) l_{q\mu} - \frac{27}{4} l_{q\mu}^2 + 6l_{q\mu}^3 \right] \right. \\ &\quad \left. + \left(\frac{\bar{m}^2}{q^2}\right)^2 \left[-\frac{885}{32} + 104\zeta_3 - 24\zeta_4 + 15\zeta_5 + 4B_4 + \left(\frac{1253}{16} - 33\zeta_3\right) l_{qm} \right. \right. \\ &\quad \left. \left. + \frac{129}{4} l_{qm}^2 + 6l_{qm}^3 + \left(\frac{195}{8} - \frac{423}{4} l_{qm} - 27l_{qm}^2\right) l_{q\mu} + \left(-\frac{189}{4} + \frac{81}{2} l_{qm}\right) l_{q\mu}^2 \right] \right. \\ &\quad \left. + \left(\frac{\bar{m}^2}{q^2}\right)^3 \left[-\frac{421657}{1944} + 135\zeta_3 - 48\zeta_4 + 80\zeta_5 + 8B_4 + \left(\frac{4481}{27} + 52\zeta_3\right) l_{qm} \right] \right\} \end{aligned}$$

$$\begin{aligned}
& + \frac{839}{6} l_{qm}^2 + \frac{1223}{27} l_{qm}^3 + \left(\frac{909}{2} - \frac{1028}{3} l_{qm} - 164 l_{qm}^2 \right) l_{q\mu} \\
& + (-192 + 144 l_{qm}) l_{q\mu}^2 \Big] \\
& + \left(\frac{\bar{m}^2}{q^2} \right)^4 \left[-\frac{159609}{128} - \frac{50}{3} \zeta_3 - 120 \zeta_4 + 280 \zeta_5 + 20 B_4 \right. \\
& + \left(\frac{751555}{1296} + 203 \zeta_3 \right) l_{qm} + \frac{534067}{864} l_{qm}^2 + \frac{38753}{216} l_{qm}^3 \\
& \left. + \left(\frac{70621}{32} - \frac{3124}{3} l_{qm} - \frac{2695}{4} l_{qm}^2 \right) l_{q\mu} + \left(-\frac{6225}{8} + \frac{1125}{2} l_{qm} \right) l_{q\mu}^2 \right] \Big\} + \dots, \tag{17}
\end{aligned}$$

$$\begin{aligned}
\bar{\Pi}_{NA}^{(2),p} = & \frac{3}{16\pi^2} \left\{ \frac{14419}{288} - \frac{75}{4} \zeta_3 - \frac{9}{8} \zeta_4 - \frac{5}{2} \zeta_5 + \left(-\frac{893}{32} + \frac{31}{4} \zeta_3 \right) l_{q\mu} + \frac{71}{12} l_{q\mu}^2 - \frac{11}{24} l_{q\mu}^3 \right. \\
& + \frac{\bar{m}^2}{q^2} \left[-\frac{25}{144} + \frac{44}{3} \zeta_3 + 3 \zeta_4 + 5 \zeta_5 + \left(\frac{153}{8} - 17 \zeta_3 \right) l_{q\mu} \right. \\
& \left. - \frac{119}{12} l_{q\mu}^2 + \frac{11}{6} l_{q\mu}^3 \right] \\
& + \left(\frac{\bar{m}^2}{q^2} \right)^2 \left[-\frac{1417}{96} + \frac{49}{4} \zeta_3 + 12 \zeta_4 + \frac{5}{2} \zeta_5 - 2 B_4 + \left(\frac{3925}{48} + \frac{15}{2} \zeta_3 \right) l_{qm} \right. \\
& \left. + \frac{38}{3} l_{qm}^2 + \frac{11}{6} l_{qm}^3 + \left(\frac{397}{24} - 49 l_{qm} - \frac{11}{2} l_{qm}^2 \right) l_{q\mu} + \left(-\frac{55}{8} + \frac{33}{4} l_{qm} \right) l_{q\mu}^2 \right] \\
& + \left(\frac{\bar{m}^2}{q^2} \right)^3 \left[-\frac{134501}{972} - \frac{63}{2} \zeta_3 + 24 \zeta_4 - 20 \zeta_5 - 4 B_4 + \left(\frac{170609}{648} - 40 \zeta_3 \right) l_{qm} \right. \\
& + \frac{497}{6} l_{qm}^2 + \frac{505}{54} l_{qm}^3 + \left(\frac{13231}{108} - \frac{3473}{27} l_{qm} - \frac{451}{18} l_{qm}^2 \right) l_{q\mu} \\
& \left. + \left(-\frac{143}{6} + 22 l_{qm} \right) l_{q\mu}^2 \right] \\
& + \left(\frac{\bar{m}^2}{q^2} \right)^4 \left[-\frac{3008885}{3888} + \frac{823}{24} \zeta_3 + 60 \zeta_4 - 70 \zeta_5 - 10 B_4 \right. \\
& + \left(\frac{1489679}{2592} - 145 \zeta_3 \right) l_{qm} + \frac{74807}{288} l_{qm}^2 + \frac{8941}{216} l_{qm}^3 \\
& \left. + \left(\frac{820055}{1728} - \frac{77761}{216} l_{qm} - \frac{5929}{72} l_{qm}^2 \right) l_{q\mu} + \left(-\frac{3905}{48} + \frac{275}{4} l_{qm} \right) l_{q\mu}^2 \right] \Big\} + \dots, \tag{18}
\end{aligned}$$

$$\begin{aligned}
\bar{\Pi}_l^{(2),p} = & \frac{3}{16\pi^2} \left\{ -\frac{511}{36} + 4 \zeta_3 + \left(\frac{65}{8} - 2 \zeta_3 \right) l_{q\mu} - \frac{11}{6} l_{q\mu}^2 + \frac{1}{6} l_{q\mu}^3 \right. \\
& \left. + \frac{\bar{m}^2}{q^2} \left[-\frac{31}{36} - \frac{4}{3} \zeta_3 + \left(-\frac{9}{2} + 4 \zeta_3 \right) l_{q\mu} + \frac{7}{3} l_{q\mu}^2 - \frac{2}{3} l_{q\mu}^3 \right] \right\}
\end{aligned}$$

$$\begin{aligned}
& + \left(\frac{\bar{m}^2}{q^2} \right)^2 \left[\frac{53}{24} - 12 \zeta_3 - \frac{257}{12} l_{qm} - \frac{10}{3} l_{qm}^2 - \frac{2}{3} l_{qm}^3 \right. \\
& \quad \left. + \left(-\frac{17}{6} + 14 l_{qm} + 2 l_{qm}^2 \right) l_{q\mu} + \left(\frac{5}{2} - 3 l_{qm} \right) l_{q\mu}^2 \right] \\
& + \left(\frac{\bar{m}^2}{q^2} \right)^3 \left[\frac{12551}{486} - \frac{16}{3} \zeta_3 - \frac{4970}{81} l_{qm} - \frac{133}{9} l_{qm}^2 - \frac{46}{27} l_{qm}^3 \right. \\
& \quad \left. + \left(-\frac{905}{27} + \frac{988}{27} l_{qm} + \frac{82}{9} l_{qm}^2 \right) l_{q\mu} + \left(\frac{26}{3} - 8 l_{qm} \right) l_{q\mu}^2 \right] \\
& + \left(\frac{\bar{m}^2}{q^2} \right)^4 \left[\frac{573913}{3888} - \frac{4}{3} \zeta_3 - \frac{13547}{81} l_{qm} - \frac{1315}{24} l_{qm}^2 - \frac{287}{54} l_{qm}^3 \right. \\
& \quad \left. + \left(-\frac{58285}{432} + \frac{5351}{54} l_{qm} + \frac{539}{18} l_{qm}^2 \right) l_{q\mu} + \left(\frac{355}{12} - 25 l_{qm} \right) l_{q\mu}^2 \right] \Big\} + \dots, \quad (19)
\end{aligned}$$

$$\begin{aligned}
\bar{\Pi}_F^{(2),p} & = \frac{3}{16\pi^2} \left\{ -\frac{511}{36} + 4 \zeta_3 + \left(\frac{65}{8} - 2 \zeta_3 \right) l_{q\mu} - \frac{11}{6} l_{q\mu}^2 + \frac{1}{6} l_{q\mu}^3 \right. \\
& \quad \left. + \frac{\bar{m}^2}{q^2} \left[\frac{161}{36} - \frac{4}{3} \zeta_3 + \left(-\frac{33}{2} + 4 \zeta_3 \right) l_{q\mu} + \frac{7}{3} l_{q\mu}^2 - \frac{2}{3} l_{q\mu}^3 \right] \right. \\
& \quad \left. + \left(\frac{\bar{m}^2}{q^2} \right)^2 \left[\frac{701}{24} + 6 \zeta_3 - \frac{293}{12} l_{qm} - \frac{11}{6} l_{qm}^2 - \frac{2}{3} l_{qm}^3 \right. \right. \\
& \quad \left. \left. + \left(-\frac{17}{6} + 14 l_{qm} + 2 l_{qm}^2 \right) l_{q\mu} + \left(\frac{5}{2} - 3 l_{qm} \right) l_{q\mu}^2 \right] \right. \\
& \quad \left. + \left(\frac{\bar{m}^2}{q^2} \right)^3 \left[\frac{43319}{486} + \frac{596}{9} \zeta_3 - \frac{3064}{27} l_{qm} - \frac{623}{27} l_{qm}^2 - \frac{92}{27} l_{qm}^3 \right. \right. \\
& \quad \left. \left. + \left(-\frac{905}{27} + \frac{988}{27} l_{qm} + \frac{82}{9} l_{qm}^2 \right) l_{q\mu} + \left(\frac{26}{3} - 8 l_{qm} \right) l_{q\mu}^2 \right] \right. \\
& \quad \left. + \left(\frac{\bar{m}^2}{q^2} \right)^4 \left[\frac{3892289}{7776} + \frac{2333}{9} \zeta_3 - \frac{20533}{72} l_{qm} - \frac{24871}{216} l_{qm}^2 - \frac{545}{27} l_{qm}^3 \right. \right. \\
& \quad \left. \left. + \left(-\frac{58285}{432} + \frac{5351}{54} l_{qm} + \frac{539}{18} l_{qm}^2 \right) l_{q\mu} + \left(\frac{355}{12} - 25 l_{qm} \right) l_{q\mu}^2 \right] \right\} + \dots, \quad (20)
\end{aligned}$$

$$\begin{aligned}
\bar{\Pi}_S^{(2),p} & = \frac{3}{16\pi^2} \left\{ \frac{\bar{m}^2}{q^2} \left[-16 \zeta_3 - 20 \zeta_5 \right] \right. \\
& \quad \left. + \left(\frac{\bar{m}^2}{q^2} \right)^2 \left[-44 + 24 \zeta_3 + (-12 - 72 \zeta_3) l_{qm} \right] \right. \\
& \quad \left. + \left(\frac{\bar{m}^2}{q^2} \right)^3 \left[\frac{221}{8} + 114 \zeta_3 + \left(-\frac{363}{4} - 36 \zeta_3 \right) l_{qm} - 63 l_{qm}^2 - 12 l_{qm}^3 \right] \right. \\
& \quad \left. + \left(\frac{\bar{m}^2}{q^2} \right)^4 \left[\frac{68146}{243} + \frac{1288}{9} \zeta_3 + \left(\frac{7727}{81} - 80 \zeta_3 \right) l_{qm} - 86 l_{qm}^2 - 44 l_{qm}^3 \right] \right\} + \dots, \quad (21)
\end{aligned}$$

The results for the one- and two-loop case have been checked against the analytical exact expressions for the polarization functions [19] in the limit of large external momentum q .

3 The decays $H \rightarrow t\bar{t}$ and $A \rightarrow t\bar{t}$

As an application of the results of the previous section we consider the decay of a scalar and pseudo-scalar Higgs boson into a top-quark pair. Thereby we neglect all light quark masses and denote the $\overline{\text{MS}}$ top quark mass by m_t and the on-shell one by M_t . Let us in a first step review the Born result and the first order QCD corrections. Taking the imaginary part of Eqs. (6) and (7) and transforming the combination $m_t^2 \bar{R}(s)$ into the on-shell scheme [16] one arrives at ($L_{ms} \equiv \ln(M_t^2/s)$)

$$R^{(0),s} = 3 \left\{ 1 - 6 \frac{M_t^2}{s} + 6 \left(\frac{M_t^2}{s} \right)^2 + 4 \left(\frac{M_t^2}{s} \right)^3 + 6 \left(\frac{M_t^2}{s} \right)^4 \right\} + \dots, \quad (22)$$

$$\begin{aligned} R^{(1),s} = & 3 \left\{ \frac{9}{4} + \frac{3}{2} L_{ms} + \frac{M_t^2}{s} \left[-6 - 18 L_{ms} \right] + \left(\frac{M_t^2}{s} \right)^2 \left[-33 + 36 L_{ms} \right] \right. \\ & \left. + \left(\frac{M_t^2}{s} \right)^3 \left[\frac{280}{9} + \frac{46}{3} L_{ms} \right] + \left(\frac{M_t^2}{s} \right)^4 \left[\frac{146}{3} + \frac{45}{2} L_{ms} \right] \right\} + \dots, \quad (23) \end{aligned}$$

for the scalar case where $\mu^2 = s$ is chosen. For the pseudo-scalar current we get from Eqs. (15) and (16):

$$R^{(0),p} = 3 \left\{ 1 - 2 \frac{M_t^2}{s} - 2 \left(\frac{M_t^2}{s} \right)^2 - 4 \left(\frac{M_t^2}{s} \right)^3 - 10 \left(\frac{M_t^2}{s} \right)^4 \right\} + \dots, \quad (24)$$

$$\begin{aligned} R^{(1),p} = & 3 \left\{ \frac{9}{4} + \frac{3}{2} L_{ms} + \frac{M_t^2}{s} \left[6 - 6 L_{ms} \right] + \left(\frac{M_t^2}{s} \right)^2 \left[-9 - 12 L_{ms} \right] \right. \\ & \left. + \left(\frac{M_t^2}{s} \right)^3 \left[-\frac{260}{9} - \frac{62}{3} L_{ms} \right] + \left(\frac{M_t^2}{s} \right)^4 \left[-\frac{674}{9} - \frac{361}{6} L_{ms} \right] \right\} + \dots. \quad (25) \end{aligned}$$

In Fig. 1 the results are plotted together with the exact expressions. For the abscissa the variable $x = 2M_t/\sqrt{s}$ is chosen. Already the approximations including only the quadratic terms provide a good agreement up to $x \approx 0.4$. It is, however, dramatically improved by incorporating higher terms in M_t^2/s , leading to an excellent approximation almost up to $x = 1$ for $R^{(0),s}$, $R^{(1),s}$ and $R^{(1),p}$ and up to $x \approx 0.85$ for $R^{(0),p}$. This serves as a strong motivation to evaluate higher order mass terms for the $\mathcal{O}(\alpha_s^2)$ corrections.

At $\mathcal{O}(\alpha_s^2)$ the results for $R^{(2),s}(s)$, separated into the contributions from the different colour factors, read in the on-shell scheme:

$$R_A^{(2),s} = 3 \left\{ \frac{109}{32} + (-6 + 6 \ln 2) \zeta_2 - \frac{15}{4} \zeta_3 + \frac{57}{16} L_{ms} + \frac{9}{8} L_{ms}^2 \right.$$

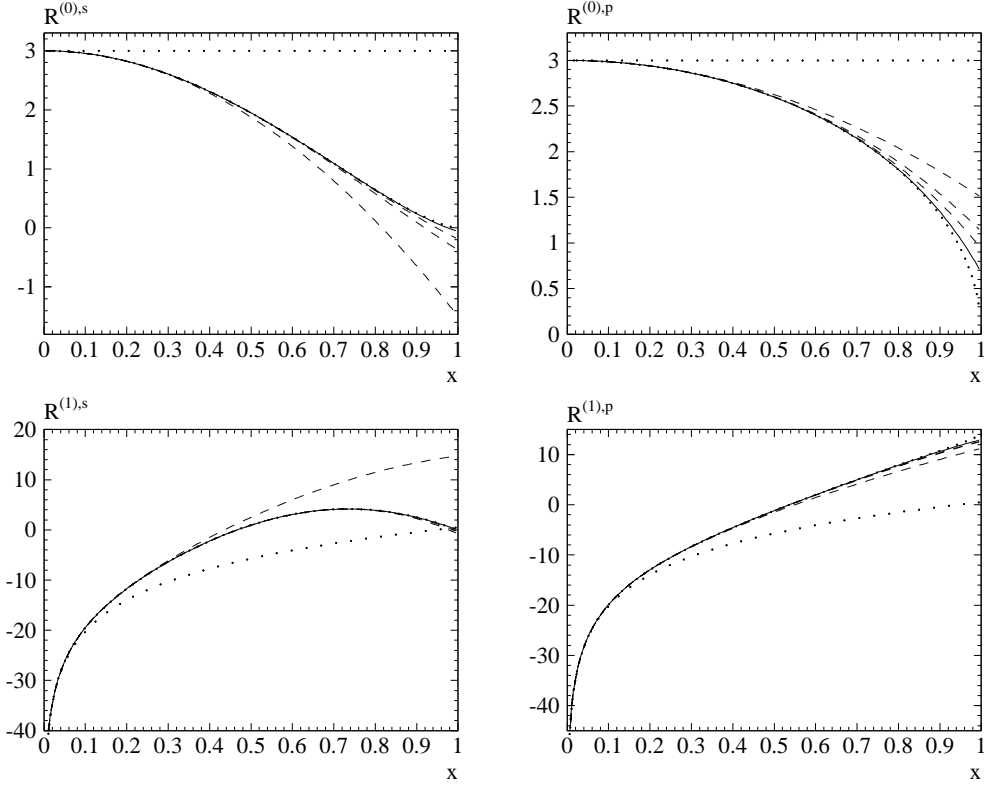


Figure 1: $R^{(0),\delta}$ and $R^{(1),\delta}$, $\delta = s, p$, plotted against $x = 2M_t/\sqrt{s}$. Successively higher order terms in $(M_t^2/s)^n$: Wide dots: $n = 0$; dashed: $n = 1, 2, 3$; solid: $n = 4$; narrow dots: exact.

$$\begin{aligned}
& + \frac{M_t^2}{s} \left[-\frac{147}{4} + (99 - 72 \ln 2) \zeta_2 + 54 \zeta_3 - \frac{81}{4} L_{ms} - 27 L_{ms}^2 \right] \\
& + \left(\frac{M_t^2}{s} \right)^2 \left[\frac{189}{2} + (-243 + 108 \ln 2) \zeta_2 - \frac{297}{2} \zeta_3 - \frac{531}{4} L_{ms} + \frac{351}{4} L_{ms}^2 \right] \\
& + \left(\frac{M_t^2}{s} \right)^3 \left[-\frac{7588}{27} + \left(-\frac{775}{9} + 96 \ln 2 \right) \zeta_2 + 34 \zeta_3 + \frac{579}{2} L_{ms} + \frac{235}{18} L_{ms}^2 \right] \\
& + \left(\frac{M_t^2}{s} \right)^4 \left[\frac{211615}{5184} + \left(-\frac{4385}{72} + 180 \ln 2 \right) \zeta_2 + \frac{83}{2} \zeta_3 \right. \\
& \quad \left. + \frac{332551}{864} L_{ms} - \frac{3715}{144} L_{ms}^2 \right] \Big\} + \dots, \tag{26}
\end{aligned}$$

$$\begin{aligned}
R_{NA}^{(2),s} &= 3 \left\{ \frac{49}{6} + \left(-\frac{3}{8} - 3 \ln 2 \right) \zeta_2 - \frac{25}{8} \zeta_3 + \frac{185}{48} L_{ms} - \frac{11}{16} L_{ms}^2 \right. \\
& \quad \left. + \frac{M_t^2}{s} \left[-\frac{317}{12} + \left(\frac{9}{2} + 36 \ln 2 \right) \zeta_2 + \frac{33}{2} \zeta_3 - \frac{185}{4} L_{ms} + \frac{33}{4} L_{ms}^2 \right] \right\}
\end{aligned}$$

$$\begin{aligned}
& + \left(\frac{M_t^2}{s} \right)^2 \left[-\frac{3253}{48} + \left(-\frac{93}{4} - 54 \ln 2 \right) \zeta_2 - \frac{61}{4} \zeta_3 + \frac{795}{8} L_{ms} - \frac{99}{8} L_{ms}^2 \right] \\
& + \left(\frac{M_t^2}{s} \right)^3 \left[\frac{75139}{1296} + \left(\frac{98}{9} - 48 \ln 2 \right) \zeta_2 + 8 \zeta_3 + \frac{1319}{27} L_{ms} - \frac{23}{2} L_{ms}^2 \right] \\
& + \left(\frac{M_t^2}{s} \right)^4 \left[\frac{391963}{3456} + \left(-\frac{17}{2} - 90 \ln 2 \right) \zeta_2 - 9 \zeta_3 \right. \\
& \quad \left. + \frac{1357}{32} L_{ms} - \frac{11}{8} L_{ms}^2 \right] \Big\} + \dots , \tag{27}
\end{aligned}$$

$$\begin{aligned}
R_l^{(2),s} & = 3 \left\{ -\frac{31}{12} + \frac{3}{2} \zeta_2 + \zeta_3 - \frac{13}{12} L_{ms} + \frac{1}{4} L_{ms}^2 \right. \\
& \quad + \frac{M_t^2}{s} \left[\frac{25}{3} - 18 \zeta_2 - 6 \zeta_3 + 13 L_{ms} - 3 L_{ms}^2 \right] \\
& \quad + \left(\frac{M_t^2}{s} \right)^2 \left[\frac{215}{12} + 33 \zeta_2 + 8 \zeta_3 - \frac{57}{2} L_{ms} + \frac{9}{2} L_{ms}^2 \right] \\
& \quad + \left(\frac{M_t^2}{s} \right)^3 \left[\frac{233}{162} + \frac{128}{9} \zeta_2 - \frac{679}{27} L_{ms} + 6 L_{ms}^2 \right] \\
& \quad \left. + \left(\frac{M_t^2}{s} \right)^4 \left[-\frac{23519}{864} + 20 \zeta_2 - \frac{2419}{72} L_{ms} + \frac{25}{2} L_{ms}^2 \right] \right\} + \dots , \tag{28}
\end{aligned}$$

$$\begin{aligned}
R_F^{(2),s} & = 3 \left\{ -\frac{13}{12} - \frac{3}{2} \zeta_2 + \zeta_3 - \frac{13}{12} L_{ms} + \frac{1}{4} L_{ms}^2 \right. \\
& \quad + \frac{M_t^2}{s} \left[-\frac{11}{3} + 18 \zeta_2 - 6 \zeta_3 + 13 L_{ms} - 3 L_{ms}^2 \right] \\
& \quad + \left(\frac{M_t^2}{s} \right)^2 \left[\frac{269}{12} - 21 \zeta_2 + 8 \zeta_3 - 27 L_{ms} + \frac{9}{2} L_{ms}^2 \right] \\
& \quad + \left(\frac{M_t^2}{s} \right)^3 \left[-\frac{53}{2} - \frac{242}{9} \zeta_2 + \frac{23}{9} L_{ms} + \frac{23}{9} L_{ms}^2 \right] \\
& \quad \left. + \left(\frac{M_t^2}{s} \right)^4 \left[-\frac{17809}{864} - \frac{71}{2} \zeta_2 + \frac{899}{24} L_{ms} - \frac{19}{4} L_{ms}^2 \right] \right\} + \dots , \tag{29}
\end{aligned}$$

$$\begin{aligned}
R_S^{(2),s} & = 3 \left\{ 12 \frac{M_t^2}{s} + \left(\frac{M_t^2}{s} \right)^2 \left[18 - 36 \zeta_3 \right] \right. \\
& \quad + \left(\frac{M_t^2}{s} \right)^3 \left[\frac{3}{8} + 36 \zeta_2 + 18 \zeta_3 + 33 L_{ms} - 18 L_{ms}^2 \right] \\
& \quad \left. + \left(\frac{M_t^2}{s} \right)^4 \left[-\frac{22289}{162} - 28 \zeta_2 - 8 \zeta_3 - 26 L_{ms} + 14 L_{ms}^2 \right] \right\} + \dots . \tag{30}
\end{aligned}$$

In the pseudo-scalar case we get:

$$\begin{aligned}
R_A^{(2),p} = & 3 \left\{ \frac{109}{32} + (-6 + 6 \ln 2) \zeta_2 - \frac{15}{4} \zeta_3 + \frac{57}{16} L_{ms} + \frac{9}{8} L_{ms}^2 \right. \\
& + \frac{M_t^2}{s} \left[-\frac{21}{4} + (33 - 24 \ln 2) \zeta_2 + 18 \zeta_3 + \frac{69}{4} L_{ms} - 9 L_{ms}^2 \right] \\
& + \left(\frac{M_t^2}{s} \right)^2 \left[50 + (81 - 36 \ln 2) \zeta_2 + \frac{51}{2} \zeta_3 - \frac{195}{4} L_{ms} - \frac{117}{4} L_{ms}^2 \right] \\
& + \left(\frac{M_t^2}{s} \right)^3 \left[\frac{3049}{54} + \left(\frac{1223}{9} - 96 \ln 2 \right) \zeta_2 - 2 \zeta_3 - \frac{459}{2} L_{ms} - \frac{683}{18} L_{ms}^2 \right] \\
& + \left(\frac{M_t^2}{s} \right)^4 \left[-\frac{672113}{5184} + \left(\frac{28223}{72} - 300 \ln 2 \right) \zeta_2 - \frac{53}{2} \zeta_3 \right. \\
& \quad \left. - \frac{518105}{864} L_{ms} - \frac{14723}{144} L_{ms}^2 \right] \left. \right\} + \dots, \tag{31}
\end{aligned}$$

$$\begin{aligned}
R_{NA}^{(2),p} = & 3 \left\{ \frac{49}{6} + \left(-\frac{3}{8} - 3 \ln 2 \right) \zeta_2 - \frac{25}{8} \zeta_3 + \frac{185}{48} L_{ms} - \frac{11}{16} L_{ms}^2 \right. \\
& + \frac{M_t^2}{s} \left[\frac{163}{12} + \left(\frac{3}{2} + 12 \ln 2 \right) \zeta_2 + \frac{11}{2} \zeta_3 - \frac{185}{12} L_{ms} + \frac{11}{4} L_{ms}^2 \right] \\
& + \left(\frac{M_t^2}{s} \right)^2 \left[-\frac{231}{16} + \left(\frac{31}{4} + 18 \ln 2 \right) \zeta_2 - \frac{33}{4} \zeta_3 - \frac{839}{24} L_{ms} + \frac{33}{8} L_{ms}^2 \right] \\
& + \left(\frac{M_t^2}{s} \right)^3 \left[-\frac{130007}{1296} + \left(\frac{26}{9} + 48 \ln 2 \right) \zeta_2 + 8 \zeta_3 - \frac{1165}{27} L_{ms} + \frac{19}{2} L_{ms}^2 \right] \\
& + \left(\frac{M_t^2}{s} \right)^4 \left[-\frac{2439823}{10368} + \left(\frac{601}{18} + 150 \ln 2 \right) \zeta_2 + 35 \zeta_3 \right. \\
& \quad \left. - \frac{97601}{864} L_{ms} + \frac{323}{24} L_{ms}^2 \right] \left. \right\} + \dots, \tag{32}
\end{aligned}$$

$$\begin{aligned}
R_l^{(2),p} = & 3 \left\{ -\frac{31}{12} + \frac{3}{2} \zeta_2 + \zeta_3 - \frac{13}{12} L_{ms} + \frac{1}{4} L_{ms}^2 \right. \\
& + \frac{M_t^2}{s} \left[-\frac{11}{3} - 6 \zeta_2 - 2 \zeta_3 + \frac{13}{3} L_{ms} - L_{ms}^2 \right] \\
& + \left(\frac{M_t^2}{s} \right)^2 \left[\frac{13}{4} - 11 \zeta_2 + \frac{61}{6} L_{ms} - \frac{3}{2} L_{ms}^2 \right] \\
& + \left(\frac{M_t^2}{s} \right)^3 \left[\frac{3851}{162} - \frac{160}{9} \zeta_2 + \frac{563}{27} L_{ms} - 6 L_{ms}^2 \right] \\
& + \left(\frac{M_t^2}{s} \right)^4 \left[\frac{199907}{2592} - \frac{460}{9} \zeta_2 + \frac{10567}{216} L_{ms} - \frac{39}{2} L_{ms}^2 \right] \left. \right\} + \dots, \tag{33}
\end{aligned}$$

$$\begin{aligned}
R_F^{(2),p} = & 3 \left\{ -\frac{13}{12} - \frac{3}{2} \zeta_2 + \zeta_3 - \frac{13}{12} L_{ms} + \frac{1}{4} L_{ms}^2 \right. \\
& + \frac{M_t^2}{s} \left[-\frac{11}{3} + 6 \zeta_2 - 2 \zeta_3 + \frac{13}{3} L_{ms} - L_{ms}^2 \right] \\
& + \left(\frac{M_t^2}{s} \right)^2 \left[-\frac{17}{4} + 7 \zeta_2 + \frac{35}{3} L_{ms} - \frac{3}{2} L_{ms}^2 \right] \\
& + \left(\frac{M_t^2}{s} \right)^3 \left[\frac{155}{6} + \frac{226}{9} \zeta_2 + \frac{113}{9} L_{ms} - \frac{31}{9} L_{ms}^2 \right] \\
& \left. + \left(\frac{M_t^2}{s} \right)^4 \left[\frac{52783}{864} + \frac{977}{18} \zeta_2 - \frac{823}{72} L_{ms} + \frac{101}{36} L_{ms}^2 \right] \right\} + \dots, \quad (34)
\end{aligned}$$

$$\begin{aligned}
R_S^{(2),p} = & 3 \left\{ \left(\frac{M_t^2}{s} \right)^2 \left[6 + 36 \zeta_3 \right] + \left(\frac{M_t^2}{s} \right)^3 \left[\frac{363}{8} - 36 \zeta_2 + 18 \zeta_3 - 63 L_{ms} + 18 L_{ms}^2 \right] \right. \\
& \left. + \left(\frac{M_t^2}{s} \right)^4 \left[-\frac{7727}{162} - 132 \zeta_2 + 40 \zeta_3 - 86 L_{ms} + 66 L_{ms}^2 \right] \right\} + \dots. \quad (35)
\end{aligned}$$

The decay width of a scalar and pseudo-scalar Higgs boson is then given by

$$\Gamma(H/A \rightarrow t\bar{t}) = \frac{G_F M_H M_t^2}{4\sqrt{2}\pi} \left[R^{s/p}(M_{H/A}^2) - C_F T \left(\frac{\alpha_s}{\pi} \right)^2 R_{gg}^{(2),s/p}(M_{H/A}^2) \right], \quad (36)$$

where $R_{gg}^{(2),\delta}$ is the contribution from the pure gluonic cut appearing in the imaginary part of the singlet diagrams which has to be subtracted if we are interested only in the fermionic final states. $R_{gg}^{(2),\delta}$ is known analytically both for the scalar [20] and pseudo-scalar case [21]. For completeness we list the expansion in M_t^2/s :

$$\begin{aligned}
R_{gg}^{(2),s}(s) = & 3 \left\{ \frac{M_t^2}{s} \left[2 + 6\zeta_2 + \frac{45}{4}\zeta_4 + \left(-1 + \frac{3}{2}\zeta_2 \right) L_{ms} + \frac{1}{8} L_{ms}^4 \right] \right. \\
& + \left(\frac{M_t^2}{s} \right)^2 \left[-24\zeta_2 - 90\zeta_4 + (-4 + 6\zeta_2) L_{ms} + (4 - 12\zeta_2) L_{ms}^2 \right. \\
& \quad \left. + L_{ms}^3 - L_{ms}^4 \right] \\
& + \left(\frac{M_t^2}{s} \right)^3 \left[-4 + 6\zeta_2 + 180\zeta_4 + (10 - 39\zeta_2) L_{ms} + (3 + 24\zeta_2) L_{ms}^2 \right. \\
& \quad \left. - \frac{13}{2} L_{ms}^3 + 2L_{ms}^4 \right] \\
& \left. + \left(\frac{M_t^2}{s} \right)^4 \left[4 - 30\zeta_2 + \left(\frac{44}{3} + 44\zeta_2 \right) L_{ms} - 15L_{ms}^2 + \frac{22}{3} L_{ms}^3 \right] \right\} + \dots, \quad (37)
\end{aligned}$$

$$R_{gg}^{(2),p}(s) = 3 \left\{ \frac{M_t^2}{s} \left[\frac{45}{4}\zeta_4 + \frac{3}{2}\zeta_2 L_{ms}^2 + \frac{1}{8} L_{ms}^4 \right] + \left(\frac{M_t^2}{s} \right)^2 \left(6\zeta_2 L_{ms} + L_{ms}^3 \right) \right\}$$

$$\begin{aligned}
& + \left(\frac{M_t^2}{s} \right)^3 \left[6\zeta_2 + 9\zeta_2 L_{ms} + 3L_{ms}^2 + \frac{3}{2}L_{ms}^3 \right] \\
& + \left(\frac{M_t^2}{s} \right)^4 \left[18\zeta_2 + (4 + 20\zeta_2) L_{ms} + 9L_{ms}^2 + \frac{10}{3}L_{ms}^3 \right] \Big\} + \dots \quad (38)
\end{aligned}$$

Note that the analytical structure is not changed if M_t is replaced by the $\overline{\text{MS}}$ mass because $R_{gg}^{(2),\delta}$ only contributes at order α_s^2 . For the numerical results presented below we only use the inclusive quantity $R^\delta(s)$.

The results for the constant and first mass corrections are in agreement with the literature both for the scalar [6, 7] and pseudo-scalar case [8]. A strong check is provided for the terms proportional to n_l where a successful comparison with the exact results for the scalar [22, 23] and pseudo-scalar [23] contributions was possible².

In Figs. 2 and 3 the contributions of the different colour factors are plotted including successively higher orders in M_t^2/s . The notation is the same as in Fig. 1. Motivated by the behavior of the Born- and one-loop terms of Fig. 1, one may consider as a measure of validity for each curve the range in x where it coincides with the one containing most powers of x (i.e., the solid line in Figs. 2 and 3). This criterion is further justified by the light fermion contribution $R_l^{(2),\delta}$, where also the exact result is known. For the scalar case, $R_l^{(2),s}$, the agreement of the exact result and the M_t^8/s^4 -terms is almost perfect up to $x = 1$, while for $R_l^{(2),p}$ the convergence above $x = 0.9$ gets poorer, but the above argument concerning the validity holds perfectly in both cases.

However, one objection is in order here, namely the fact that $R_A^{(2),\delta}$, $R_{NA}^{(2),\delta}$, $R_F^{(2),\delta}$ and $R_S^{(2),\delta}$, in contrast to $R_l^{(2),\delta}$, exhibit a four-particle threshold at $x = 1/2$ which may spoil convergence for $x > 1/2$. Indeed, the curves for $R_F^{(2),\delta}$, $R_S^{(2),\delta}$ (Fig. 3) develop a relatively large spread in this x -range. Nevertheless, the range of validity as defined above extends to $x = 0.7 - 0.8$. Despite this objection, the curves for $R_{NA}^{(2),\delta}$ seem to converge very well again almost up to $x = 1$, those for $R_A^{(2),\delta}$ at least up to $x \approx 0.85$. In particular for the scalar case, where the exact result is known to be zero³ at $x = 1$, the behavior of the approximations is quite promising.

Summarizing, one can see that while the quadratic mass terms seem to reasonably approximate the result up to $x = 0.3 - 0.4$ for the scalar and $x \approx 0.5$ for the pseudo-scalar case, the quartic terms considerably improve the expansions in most cases up to values of $x \approx 0.85$, in some cases even up to $x = 1$. The influence of the higher order terms is rather small and practically only needed for $R_A^{(2),\delta}$ and $R_S^{(2),\delta}$.

It is interesting to compare the results both for the on-shell and the $\overline{\text{MS}}$ -definition of the quark mass. Therefore we set $\mu^2 = s$ which is the natural choice because it eliminates all logarithms of the constant and quadratic terms in the $\overline{\text{MS}}$ scheme. Starting from the quartic term, however, $\ln M_t^2/s$ terms remain, resulting from non-trivial operators which are absent before [24]. In contrast to the $\overline{\text{MS}}$ scheme the results in the on-shell scheme develop $\ln M_t^2/s$ terms starting from the lowest order. It is nevertheless instructive to

²We would like to thank the authors of [23] for providing us with the results prior to publication.

³ $R_S^{(2),s} \neq 0$ because the gluon cut is still present.

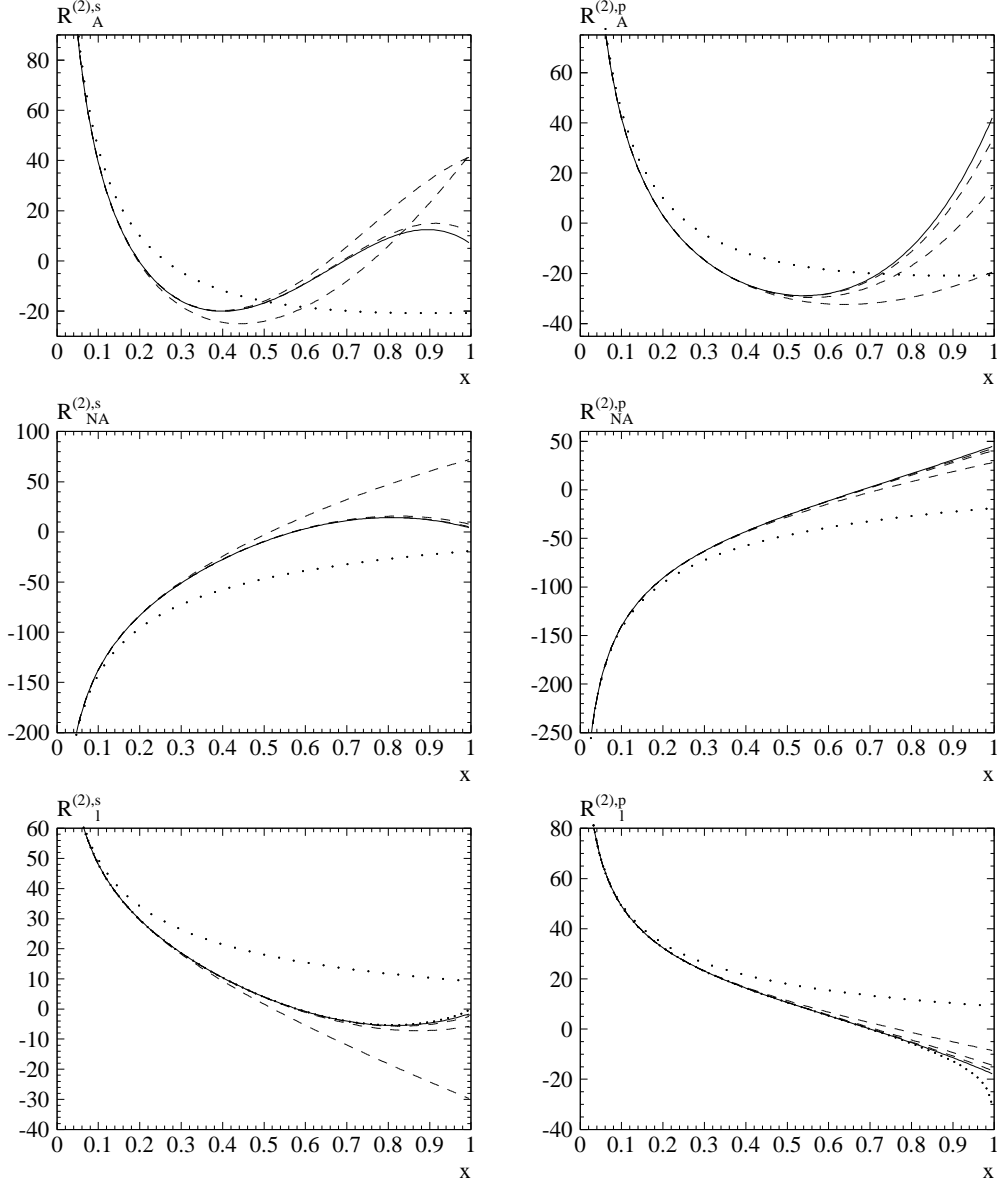


Figure 2: $R_n^{(2),\delta}$ with $\delta = s, p$ and $n = A, NA, l$ plotted against x . The same notation as in Fig. 1 is adopted.

compare the expansions both in M_t^2/s and $\alpha_s(s)$ in the two schemes. Therefore the renormalization group invariant quantities $m_t^2(s)\bar{R}^\delta(s)/M_t^2$ and $R^\delta(s)$ are considered. We choose $n_l = 5$, $\alpha_s^{(5)}(M_Z^2) = 0.118$, $M_t = 175$ GeV and $M_{H/A} = 450$ GeV which corresponds to $x \approx 0.78$. The corresponding $\overline{\text{MS}}$ top mass, $m_t(M_{H/A})$, evaluates to $m_t(450 \text{ GeV}) = 155$ GeV and the two-loop beta function leads to $\alpha_s((450 \text{ GeV})^2) \equiv \alpha_s^{(6)}((450 \text{ GeV})^2) \approx 0.096$. In Tab. 1 the numbers are listed. It can be seen that the quartic terms are still

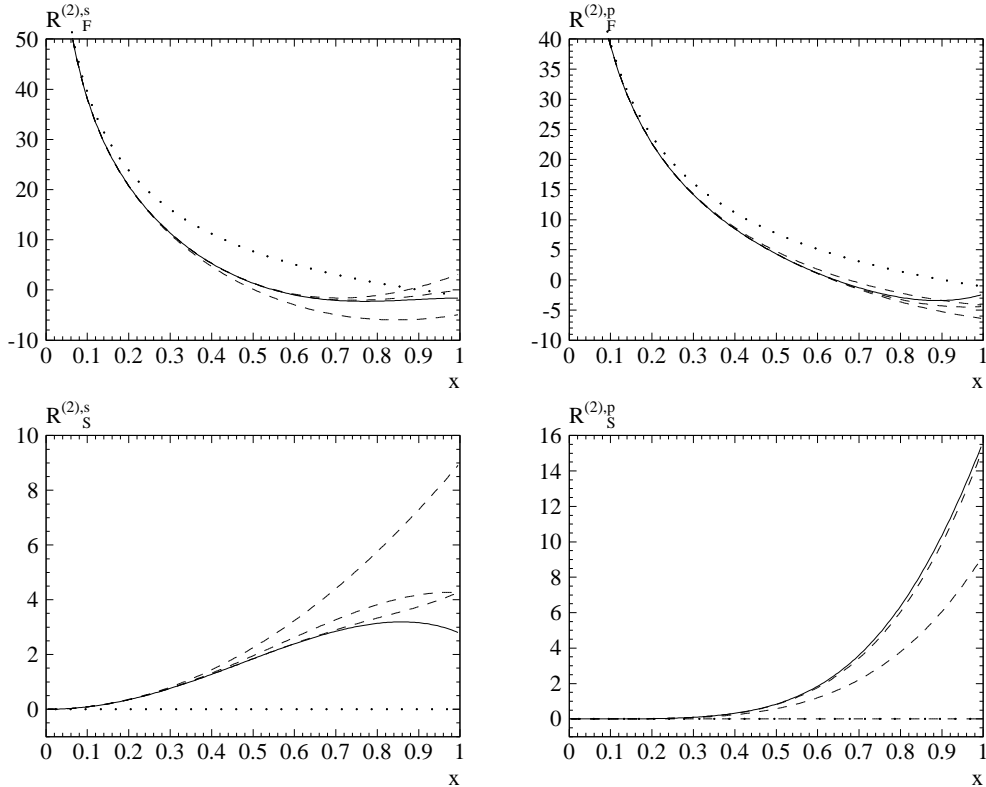


Figure 3: $R_n^{(2),\delta}$ with $\delta = s, p$ and $n = F, S$ plotted against x . The same notation as in Fig. 1 is adopted.

sizeable and in many cases numerically of the same order as the constant and quadratic ones. They become particularly important when the first two terms happen to cancel to a large extent. The higher order terms give only small contributions at least in the three-loop case.

Usually in the $\overline{\text{MS}}$ scheme a faster convergence of the QCD series is expected in the sense that the coefficients in front of $(\alpha_s/\pi)^n$ are smaller than in the on-shell scheme. Considering the sum of all approximation terms available this happens to be true only for the scalar correlator whereas in the pseudo-scalar case it is vice versa. A possible explanation might be that the coefficient of the leading term in the on-shell scheme is already rather small because of an accidental cancellation between the constant and the logarithm. For the scalar correlator there is in addition a large cancellation between the first three terms in the $\overline{\text{MS}}$ scheme so that the sum turns out to be also rather small. This is not the case for R^p where the first three terms have the same sign. However, the scheme dependence is drastically reduced by the inclusion of the $\mathcal{O}(\alpha_s^2)$ terms as can be seen in Tab. 1.

Finally we want to present numerical values for the physical decay rate into top quarks.

	$(M_t^2)^0$	$(M_t^2)^1$	$(M_t^2)^2$	$(M_t^2)^3$	$(M_t^2)^4$	Σ	exact
scalar, on-shell							
$R^{(0),s}/3$	1.000	-0.907	0.137	0.014	0.003	0.247	0.248
$C_F R^{(1),s}/3$	-0.778	5.646	-3.080	0.010	0.004	1.802	1.802
$R^{(2),s}/3$	-35.803	77.056	-17.792	-5.347	-0.680	17.435	-
$\Sigma_i(\alpha_s/\pi)^i$	0.943	-0.663	0.026	0.009	0.003	0.318	
scalar, $\overline{\text{MS}}$							
$\frac{m_t^2}{M_t^2} \bar{R}^{(0),s}/3$	0.784	-0.558	0.066	0.005	0.001	0.298	0.299
$\frac{m_t^2}{M_t^2} C_F \bar{R}^{(1),s}/3$	4.445	-3.723	-0.238	0.143	0.032	0.659	0.673
$\frac{m_t^2}{M_t^2} \bar{R}^{(2),s}/3$	21.799	-7.606	-15.334	0.680	0.546	0.086	-
$\Sigma_i(\alpha_s/\pi)^i$	0.941	-0.679	0.045	0.010	0.002	0.319	
pseudo-scalar, on-shell							
$R^{(0),p}/3$	1.000	-0.302	-0.046	-0.014	-0.005	0.633	0.629
$C_F R^{(1),p}/3$	-0.778	3.495	0.417	0.047	0.027	3.208	3.238
$R^{(2),p}/3$	-35.803	25.024	12.173	3.780	1.293	6.467	-
$\Sigma_i(\alpha_s/\pi)^i$	0.943	-0.172	-0.022	-0.009	-0.003	0.737	
pseudo-scalar, $\overline{\text{MS}}$							
$\frac{m_t^2}{M_t^2} \bar{R}^{(0),p}/3$	0.784	-0.186	-0.022	-0.005	-0.002	0.569	0.569
$\frac{m_t^2}{M_t^2} C_F \bar{R}^{(1),p}/3$	4.445	-0.248	-0.215	-0.119	-0.043	3.821	3.791
$\frac{m_t^2}{M_t^2} \bar{R}^{(2),p}/3$	21.799	9.854	2.455	-0.781	-0.520	32.807	-
$\Sigma_i(\alpha_s/\pi)^i$	0.941	-0.185	-0.026	-0.010	-0.003	0.717	

Table 1: Numerical results for R^s and R^p both in the on-shell and $\overline{\text{MS}}$ scheme. The contributions from the mass terms $(M_t^2)^i$, their sum (Σ) and, where available, the exact results are shown. $\Sigma_i(\alpha_s/\pi)^i$ is the sum of the 1-, 2- and 3-loop terms. The numbers correspond to $M_t = 175$ GeV and $M_{H/A} = 450$ GeV. The renormalization scale μ^2 is set to $s = M_{H/A}^2$.

For convenience the square of the on-shell mass, M_t^2 , is factored out both in the on-shell and $\overline{\text{MS}}$ scheme. Using Eq. (36) the expansions of the decay width for the scalar and pseudo-scalar case look like:

$$\Gamma(H \rightarrow t\bar{t}) = \frac{G_F M_H M_t^2}{4\sqrt{2}\pi} [0.7404 + 0.1652 + 0.0469 + 0.0019 - 0.0022], \quad (39)$$

$$\bar{\Gamma}(H \rightarrow t\bar{t}) = \frac{G_F M_H M_t^2}{4\sqrt{2}\pi} [0.8954 + 0.0604 - 0.0011 + 0.0014 - 0.0020], \quad (40)$$

$$\Gamma(A \rightarrow t\bar{t}) = \frac{G_F M_H M_t^2}{4\sqrt{2}\pi} [1.8982 + 0.2941 + 0.0146 + 0.0035 - 0.0051], \quad (41)$$

$$\bar{\Gamma}(A \rightarrow t\bar{t}) = \frac{G_F M_H M_t^2}{4\sqrt{2}\pi} [1.7084 + 0.3503 + 0.0903 + 0.0016 - 0.0038], \quad (42)$$

where the first and second number correspond to the Born and $\mathcal{O}(\alpha_s)$ correction. The $\mathcal{O}(\alpha_s^2)$ terms are separated into the non-singlet (third number) and singlet (fourth number) contribution. The last number corresponds to the gluonic cut which has to be subtracted. The last two numbers cancel each other to a large extent which means that the two-gluon-cut dominates the imaginary part of the double-triangle diagram. Furthermore one observes that the two-loop QCD corrections amount up to $\approx 5\%$.

To conclude, we have computed analytically the first five terms of the scalar and pseudo-scalar current correlator in the expansion for large external momentum q . As an application the decay of a scalar and pseudo-scalar Higgs boson into top quarks is considered. In this case the higher order mass corrections, especially the quartic terms, emerge to be important.

Acknowledgments

We would like to thank K.G. Chetyrkin and J.H. Kühn for fruitful discussions and for carefully reading the manuscript. M.S. would like to thank P. Gambino for useful discussions. The work of R.H. was supported by the ‘‘Landesgraduiertenförderung’’ at the University of Karlsruhe.

References

- [1] P. Janot, in *Proceedings of the Ringberg Workshop: The Higgs puzzle—What can we learn from LEP 2, LHC, NLC, and FMC?*, Tegernsee, Germany, 8–13 December 1996, edited by B.A. Kniehl (World Scientific, Singapore, to appear).
- [2] M. Boutemeur, in Ref. [1].
- [3] G. Degrandi, P. Gambino and A. Sirlin; Report Nos. MPI/PhT/96-118, NYU-TH-96-11-02 and hep-ph/9611363.
- [4] M. Drees and K. Hikasa, *Phys. Lett. B* **240** (1990) 455; erratum-ibid. **B 262** (1991) 497.
- [5] S.G. Gorishny, A.L. Kataev, S.A. Larin and L.R. Surguladze *Mod. Phys. Lett. A* **5** (1990) 2703; *Phys. Rev. D* **43** (1991) 1633.
- [6] L.R. Surguladze, *Phys. Lett. B* **341** (1994) 60.
- [7] K.G. Chetyrkin and A. Kwiatkowski, *Nucl. Phys. B* **461** (1996) 3.
- [8] L.R. Surguladze, *Phys. Lett. B* **338** (1994) 229.

- [9] K.G. Chetyrkin, *Phys. Lett.* **B 390** (1997) 309.
- [10] K.G. Chetyrkin, R. Harlander, J.H. Kühn and M. Steinhauser, in *Proceedings of the 5th International Workshop on New Computing Techniques in Physics Research: Software Engineering, Neural Nets, Genetic Algorithms, Expert Systems, Symbolic Algebra, Automatic Calculations (AIHENP 96)*, Lausanne, Switzerland, 2–6 September 1996; Report Nos. MPI/PhT/96-122, TTP96-55 and hep-ph/9611354.
- [11] K.G. Chetyrkin, R. Harlander, J.H. Kühn and M. Steinhauser, Report Nos. MPI/PhT/97-12, TTP97-11 and hep-ph/9704222.
- [12] For a review see e.g.: V.A. Smirnov, *Mod. Phys. Lett.* **A 10** (1995) 1485.
- [13] J.A.M. Vermaseren, *Symbolic Manipulation with FORM*, (Computer Algebra Netherlands, Amsterdam, 1991).
- [14] S.A. Larin, F.V. Tkachov and J.A.M. Vermaseren, Preprint NIKHEF-H/91-18 (1991).
- [15] D.J. Broadhurst, *Z. Phys.* **C 54** (1992) 54.
- [16] N. Gray, D.J. Broadhurst, W. Grafe, and K. Schilcher, *Z. Phys.* **C 48** (1990) 673.
- [17] G. 't Hooft and M. Veltman, *Nucl. Phys.* **B 44** (72) 189;
P. Breitenlohner and D. Maison, *Comm. Math. Phys.* **52** (1977) 11.
- [18] S.A. Larin, *Phys. Lett.* **B 303** (1993) 113.
- [19] A. Djouadi and P. Gambino, *Phys. Rev.* **D 51** (1995) 218; erratum-ibid. **D 53** (1996) 4111;
D.J. Broadhurst, *Phys. Lett.* **B 101** (1981) 423.
- [20] J. Ellis, M.K. Gaillard, and D.V. Nanopoulos, *Nucl. Phys.* **B 106** (1976) 292.
- [21] A. Djouadi, M. Spira, and P.M. Zerwas, *Phys. Lett.* **B 311** (1993) 255.
- [22] K. Melnikov, *Phys. Rev.* **D 53** (1996) 5020.
- [23] A.H. Hoang and T. Teubner, *private communication*.
- [24] D.J. Broadhurst and S.C. Generalis, Preprint OUT-4102-12, (1984);
K.G. Chetyrkin and V.P. Spiridonov, *Yad. Fiz.* **47** (1988) 818; *Sov. J. Nucl. Phys.* **47** (1988) 522.